The Role of Nonlinear Dynamics in Affective Valence and Arousal Recognition

Gaetano Valenza, *Student Member*, *IEEE*, Antonio Lanatà, *Member*, *IEEE*, and Enzo Pasquale Scilingo, *Member*, *IEEE*

Abstract—This paper reports on a new methodology for the automatic assessment of emotional responses. More specifically, emotions are elicited in agreement with a bidimensional spatial localization of affective states, that is, arousal and valence dimensions. A dedicated experimental protocol was designed and realized where specific affective states are suitably induced while three peripheral physiological signals, i.e., ElectroCardioGram (ECG), ElectroDermal Response (EDR), and ReSPiration activity (RSP), are simultaneously acquired. A group of 35 volunteers was presented with sets of images gathered from the International Affective Picture System (IAPS) having five levels of arousal and five levels of valence, including a neutral reference level in both. Standard methods as well as nonlinear dynamic techniques were used to extract sets of features from the collected signals. The goal of this paper is to implement an automatic multiclass arousal/valence classifier comparing performance when extracted features from nonlinear methods are used as an alternative to standard features. Results show that, when nonlinearly extracted features are used, the percentages of successful recognition dramatically increase. A good recognition accuracy (> 90 percent) after 40-fold cross-validation steps for both arousal and valence classes was achieved by using the Quadratic Discriminant Classifier (QDC).

Index Terms—Emotion recognition, affective computing, nonlinear analysis, feature extraction.

1 Introduction

Common experience suggests that emotions cannot be reduced to single word definitions. Researchers exploring the subjective experience of emotion have pointed out that emotions are highly intercorrelated both within and between the subjects reporting them [1], [2]. For example, subjects rarely describe feeling a specific positive emotion without also claiming to feel other positive emotions [3]. This high variability in expression and definition of emotions implies that the development of an automatic emotion-recognition-system is a very challenging task. In this context three crucial issues have to be addressed: modeling, elicitation, and classification of emotions. In the next sections they are described in detail.

1.1 Modeling Emotions

In the literature, several approaches for modeling emotions have been proposed. Discrete, dimensional, appraisal, and dynamical models are the most interesting, and in addition, they are not exclusive of each other.

In *discrete models*, emotions can be seen as the result of a selective adaptation that ensures survival [4]. This survival concept could be illustrated by the following relation: $\mathrm{danger}{=>}\mathrm{fear}{=>}\mathrm{escape}{=>}\mathrm{survival}$. The result of this selection is a small set of basic, innate, and universal emotions. For instance, Ekman proposed six basic emotions which are identified on the basis of facial expressions: anger, disgust, fear, joy, sadness, and surprise [5], [6]. Besides, in the literature other discrete models have been proposed which include more or less basic emotions, usually from 2 to 10 ([7], [8], [9]). These emotions are called primary emotions as opposed to secondary emotions which result from a combination of the primary ones (e.g., contempt = anger + disgust). Nevertheless, this model can be insufficient to describe mixed emotions, which necessarily require much more than one word to be expressed, and in addition there are some controversies in the assumption of the universality of basic emotions (Darwinian hypothesis [4]). What seems true is that emotions are universally expressed (facial expressions [10]), but dependent on semantic attributions. It shows that intercultural differences, e.g., difference between Asian and Occidental people, are more important than intracultural differences, e.g., between genders, and that no significant difference between primary and secondary emotions exists. From an evolutionary point of view, basic emotions may be the first emotions infants could experience [11]. See Ortony and Turner [12] for basic emotion categories defined over the years.

Unlike discrete models, *dimensional models* consider a continuous multidimensional space where each dimension stands for a fundamental property common to all emotions. This kind of model has already been used by Wundt [13]. Over the years, a large number of dimensions have been proposed [14], [15], [16], [17], [18], [19]. Two of the most accepted dimensions were described by Russel [20]: valence (i.e., pleasure, positive versus negative affect) and arousal (low versus high level of activation). These dimensions were derived from Valence, Arousal, and Dominance (PAD) space

• *The authors are with the Interdepartmental Research Center "E. Piaggio," University of Pisa, via Diotisalvi 2, 56126 Pisa, Italy. E-mail: gaetano.valenza@iet.unipi.it, a.lanata@centropiaggio.unipi.it, e.scilingo@ing.unipi.it.*

Manuscript received 4 Apr. 2011; revised 15 July 2011; accepted 9 Aug. 2011; published online 24 Aug. 2011.
Recommended for acceptance by J.-M. Fellous.
For information on obtaining reprints of this article, please send e-mail to: taffc@computer.org, and reference IEEECS Log Number TAFFC-2011-04-0029.
Digital Object Identifier no. 10.1109/T-AFFC.2011.30.

developed by Russell and Mehrabian [21], in which dominance represents the degree of control over the situation.

Appraisal models are based on the evaluation of current, remembered, or imagined circumstances. At the heart of appraisal theory is the idea that the particular judgments made about the environment and ourselves cause different emotions. The situational appraisals appear to be highly dependent on motives and goals. In other words, how we feel depends on what is important to us; indeed, all our appraisals are connected to what we want and therefore to how we feel. For example, frustration results from a goal which is not achieved. This model was introduced by Arnold [22] and has been developed and refined by Frijda [23], Ortony et al. by developing the OCC model [24], Scherer with the Component Process Theory (CPT) [25], and the derived one by Lisetti and Gmytrasiewicz [26].

The appraisal process can be thought of as having a continuous as well as a categorical nature. Roseman's (1996) model shows that appraisal information can vary continuously, but categorical boundaries determine which emotion will occur. To solve the problem between categorical and continuous appraisal order, it may be a good idea to place discrete emotional categories (i.e., happiness, sadness, etc.) while continuous models represent the varieties, styles, and levels of these already defined distinct emotions [27]. Finally, the *dynamical model* approach considers emotions as a dynamical process. This model starts from an evolutionary perspective and characterizes emotion in terms of response tendencies. In the dynamics perspective, emotion is a regulable system and the capability of understanding its rules is essential. According to a process model of emotion regulation, emotion may be regulated at five points in the emotion generative process: selection of the situation, modification of the situation, deployment of attention, change of cognitions, and modulation of responses. It may be useful to take into account concepts like mood and personality (see Egges et al. for an implemented model [28]).

In this work, we adopted a common dimensional model which uses multiple dimensions to categorize emotions, the Circumplex Model of Affects (CMA) [29]. This model interprets emotional mechanisms underlying affects as a continuum of highly interrelated and often ambiguous states. They are distributed on a Cartesian system of axes; Each axis represents a neurophysiological pathway by which emotion is being processed. In many cases, by using factor analysis and multidimensional scaling of a wide set of psychometric assessments and self-reports on emotional states, it is possible to use a more simplified bidimensional model. In particular, in the CMA used in our experiments the two dimensions are conceptualized by the terms of valence and arousal, which can be intended as the two independent, predominantly subcortical systems that underlie emotions (see Fig. 1). Valence represents how much an emotion is felt by people as positive or negative. For example, someone feeling sad has evaluated surrounding events as very negative. On the contrary, someone feeling joy would have appraised the environment as positive for his well being. Arousal indicates how relevant the surrounding events are and therefore how strong the emotion is. In this case, someone feeling excited will have an emotion represented by a bigger arousal and someone feeling bored will experience a much less relevant emotion. Accordingly, in CMA, arousal and valence can be considered adequate parameters to identify specific emotions. This simplified model addresses most of the methodological issues raised by experimental studies on emotions and provides a reliable means for comparing outcomes.

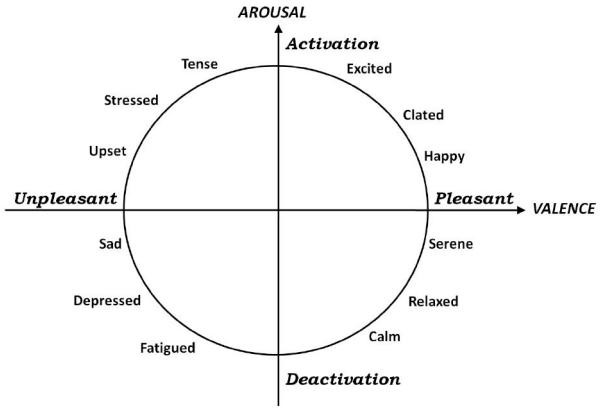

Fig. 1. A graphical representation of the circumplex model of affect with the horizontal axis representing the valence dimension and the vertical axis representing the arousal or activation dimension.

1.2 Emotion Elicitation

How emotions can be elicited is a crucial issue still open. Several modalities and several perceptual channels could be used for this purpose, which can be thought as affected by several "noisy" factors, including physiological process such as attention, social interaction, and body-to-biosensors connections. Since this work aims at discriminating emotions by processing the Autonomic Nervous System (ANS) responses upon a suitable elicitation process, noisy factors could worsen the capability to recognize differences between affective states.

In the literature, a wide range of elicitation methods have been applied: introspection, movements, lights, and colors [30], set of actions, images (e.g., IAPS described below) [31], sounds (e.g., music and IADS described below) [32], [33], [34], (fragments of) movies [35], [36], speech [37], commercials [38], games, agents/serious gaming/virtual reality [39], reliving of emotions [40], and real-world experiences [41], [42].

Some of these methods, in order to induce a specific emotion, employ stimuli belonging to international standardized database. In this perspective, the International Affective Picture System (IAPS) [43] and the International Affective Digital Sounds system (IADS) [44] are two of the most frequently cited tools in the area of affective stimulation. They consist of hundreds of images and sounds, with associated standardized affective values. A commonly used approach is to have a collection of stimuli in which each is slightly varied in terms of intra-individual standard deviation of affective ratings.

In our experiments, a set of images gathered from the IAPS is chosen [45]. The IAPS is a set of 944 images having a specific emotional rating in terms of valence, arousal, and dominance. The emotional ratings are based on several

TABLE 1
Performance of the Peripheral Biosignal-Based Emotion Recognition Methods Reported in the Literature of the Last Decade

Author	Signals	Elicitation	Emotion Classes	Classification	Best results (%)
Picard et al. 2001 [49]	EMG, BVP, EDR, RSP	Internal feeling of each emotion	Neutral, anger, hatred, grief, platonic love, romantic love, joy, reverence	LDA	81.0
Lisetti and Nasoz 2004 [50]	ECG, EDR, ST	Film Clips and difficult mathematics questions	sadness, anger, fear, surprise, frustration, and amusement	MBA	84
Haag et al. 2004 [51]	EMG, EDR, ST, BVP, ECG, RSP	IAPS	Valence	ANN	90
			Arousal		96
Kim et al 2004 [52]	ECG, ST, EDR	Audio, Visual and Cognitive stimuli	Sadness, anger, stress, surprise	SVM	61.8
Yoo et al. 2005 [53]	ECG, EDR	Video clip	Sad, Calm pleasure, Interesting pleasure, Fear	ANN	80
Choi & Woo et al 2005 [54]	BVP, EDR	Music and image choosen by subject	joy, anger, and sadness	ANN	74.5
Healey & Picard 2005 [42]	EMG, ECG, EDR, RSP	Driving	3 Stress Levels	LDA	97
Li & Chen 2006 [55]	ECG, BVP, EDR, ST	Film Clips	Fear, neutral, and joy	CCA	93.33
Rani et al. 2006 [56]	ECG, BVP, EDR, EMG	Cognitive tasks (i.e. Anagrams and Pong)	engagement, anxiety, boredom, frustration and anger	SVM	86
Rainville et.al. 2006 [57]	ECG, RSP, EDR, EMG	Self Induction	Anger, Fear, Happiness, Sadness	SDA	49
Zhai & Barreto 2006 [58]	EDR, BVP, PD, ST	Stroop Test game	2 stress levels	SVM	90
Leon et al. 2007 [39]	ECG, EDR, BVP	IAPS	Neutral, Negative, Positive	ANN	71
Liu et al. 2008 [59]	ECG, ICG, BVP, HS, EDR, EMG, ST	Cognitive tasks (i.e. anagrams and Pong.)	Anxiety, Engagement, Liking.	SVM	83
Katsis et al 2008 [60]	EMG, ECG, RSP, EDR	Car-racing drivers	High stress, low stress, disappointment, euphoria	SVM	79.3
Yannakakis & Hallam 2008 [61]	ECG, BVP, EDR	Interactive Games	2 fun levels	SVM, ANN	70
Kim & Andrè 2008 [32]	EMG, ECG, EDR, RSP	Music Listening	4 Musical Emotion	LDA	70/95
Katsis et al. 2010 [62]	BVP, ECG, EDR, RSP	IAPS	Relaxed, neutral, startled, apprehensive, very apprehensive	ANN, SVM	84

studies previously conducted where subjects were requested to rank these images using the Self Assessment Manikin [46]. In addition, the elicitation by IAPS is able to activate segregated neural representations of the different emotion dimensions in different prefrontal cortical regions [47], [48]. Five classes of arousal and five valence levels were selected and presented to 35 healthy subjects in a controlled environment in the form of a slideshow.

1.3 From Theory to Emotion Recognition

An automatic emotion recognition system requires the following stages: emotion elicitation, acquisition and processing of bioinformation, training, and classification of emotional features. The bioinformation includes implicit emotional channels of human communication, such as speech, facial expression, gesture, physiological responses, etc. Recently, numerous studies based on engineering approaches to automatically recognize emotions have been published. After a detailed study of the state of the art, we summarized into an extensive survey-table (see Table 1), the most relevant results reported in the literature during the last decade about the emotion recognition through the peripheral biosignal response [49], [50], [51], [52], [53], [54], [42], [55], [56], [57], [58], [39], [59], [60], [61], [32], [62]. All the acronyms used in this table are expanded in Table 2. Each row of Table 1 shows the first author along with the publication year, the set of physiological signals used for that study, the typology of stimulation pattern, the emotion

TABLE 2
Peripheral Biosignals and Classification Methods Used in the Literature, along with Acronyms

Peripheral Biosignals	Acronym
ElectroCardioGram	ECG
ElectroMyoGram	EMG
Blood Volume Pulse	BVP
ElectroDermal Response	EDR
ReSPiration Activity	RSP
Skin Temperature	ST
Pupil Diameter	PD
Impedance CardioGram	ICG
Heart Sound	HS
Classification methods	**Acronym**
Linear Discriminant Analysis	LDA
Marquardt Backpropagation Algorithm	MBA
Artificial Neural Network	ANN
Support Vector Machine	SVM
Canonical Correlation Analysis	CCA
Step wise Discriminant Analysis	SDA

TABLE 3
Rating of IAPS Images Used in This Work

Session	N. Images	Valence Rating	Valence Range	Arousal Rating	Arousal Range
Neutral	6	6.49±0.87	5.52÷7.08	2.81±0.24	2.42÷3.22
Arousal 1	20	/	2.87÷7.63	3.58±0.30	3.08÷3.98
Arousal 2	20	/	1.95÷8.03	4.60±0.31	4.00÷4.99
Arousal 3	20	/	1.78÷7.57	5.55±0.28	5.01÷6.21
Arousal 4	20	/	1.49÷7.77	6.50±0.33	5.78 ÷6.99

classes, the type of the classifier, and the results in terms of best percentage of successful recognition. This work focuses on identifying valence and arousal levels by estimating changes in the sympatho-vagal balance by acquiring and processing a minimal set of peripheral physiological signals.

More specifically, three biosignals were gathered: ElectroCardioGram (ECG), ReSPiration (RSP) signal, and ElectroDermal Response (EDR). A set of features extracted by these signals was then used to implement an automatic-emotion-recognition system. In particular, we extracted commonly used standard features and features from nonlinear dynamic methods of analysis. The arousal and valence multiclass recognition was performed by processing the extracted feature sets through a Bayesian decision theory based classifier which used a Quadratic Discriminant function (QDC). Experimental results are shown in the form of confusion matrices [63] in which standard feature sets and feature sets from nonlinear dynamic techniques were compared. All the algorithms were implemented by using Matlab v7.2 with a support for classifiers by using the routines available in the well-known Matlab toolbox for pattern recognition (PRTool) [64], Time Series Analysis Toolbox [65]. In this paper, we will describe the experimental protocol, and the methodologies of signal processing, feature extraction, feature reduction, and classification. Finally, experimental results will be shown and discussed.

2 Experimental Protocol

In this work, a protocol for reliability and reproducibility of experiments was designed and a hardware integrated-system able to acquire and elaborate physiological signals along with a suitable visual stimulus elicitation system was realized. The protocol was structured into the following phases: recruitment of eligible subjects, affective state elicitation, acquisition of the physiological signal set.

2.1 Recruitment of Eligible Subjects

A group of 35 healthy subjects, i.e., not suffering from both cardiovascular and evident mental pathologies, was recruited to participate in the experiment. Their age ranged from 21 to 24 and the were naive to the purpose of the experiment. All participants were screened by Patient Health Questionnaire (PHQ) and only participants with a score lower than 5 were included in the study. The cutoff value was chosen in order to avoid the presence of either middle or severe personality disorders [66]. The test uses an empirical keying approach, where scales of personality were derived from items endorsed by patients. It consists of 16 items, and usually took between 20 and 30 minutes (depending on reading level). The test was presented in the Italian language as the subjects were native Italian speakers.

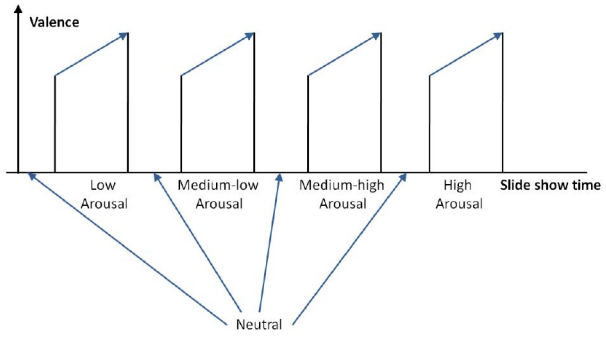

Fig. 2. Sequence scheme over time of image presentation. The y-axis relates to $Valence$.

2.2 Stimulus Elicitation

The affective elicitation was performed by projecting a set of images to a PC monitor. These images were chosen from the official IAPS database. In this work, the slideshow was projected in a room equipped with a dedicated monitor and headset to acoustically insulate from external noise. The slideshow was comprised of nine sessions of images $N, A1, N, A2, N, A3, N, A4, N$, where N is a session of six neutral images (mean valence rating 6.49, $SD = 0.87$, $\text{range} = 5.52 \div 7.08$; $\text{mean arousal rating} = 2.81$, $SD = 0.24$, $\text{range} = 2.42 \div 3.22$) , and A_i (with i going from 1 to 4) are sets of 20 images eliciting an increasing level of arousal and valence. Detailed values are reported in Table 3. The overall protocol utilized 110 images. Each image was presented for 10 seconds for a total duration of the experiment of 18 minutes and 20 seconds. Fig. 2 shows a graphical representation of the protocol. During the visual elicitation three physiological signals, ECG, RSP, and EDR, were acquired.

2.3 Set of Physiological Signals and Instrumentation

The physiological signals were acquired simultaneously by using the BIOPAC MP150 with three biosensors: ECG, RSP, and EDR. The sampling rate is 250 Hz for all signals.

2.3.1 ECG

We used the ECG100C Electrocardiogram Amplifier from BIOPAC Inc., which records the D2 lead ECG signal (bandwidth: 0.05-35 Hz) connected with pregelled Ag/AgCl electrodes placed following Einthoven triangle configuration. ECG signal was used to extract the HRV [67], which reflects the sympathetic-parasympathetic balance. HRV refers to the variation of the time interval between consecutive heartbeats.

2.3.2 Respiration

The dedicated module of BIOPAC MP150 used to record the respiration activity is RSP100C Respiration Amplifier with the TSD201 sensor, which is a piezoresistive sensor with the output resistance within the range $5 \div 125$ KOhm and bandwidth of $0.05 \div 10$ Hz. This piezoresistive sensor changed its electrical resistance if stretched or shortened, and it was sensitive to the thoracic circumference variations occurring during respiration [68].

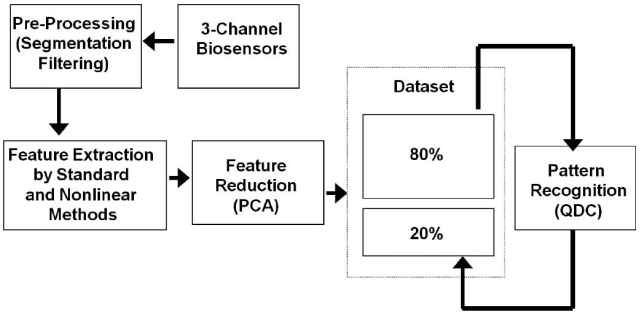

Fig. 3. Block diagram representing the acquisition and processing chain.

2.3.3 Electrodermal Response

EDR represents changes in the skin's electrical properties, i.e., electric impedance, due to psychologically induced sweat gland activity [69] upon an external stimulus. More specifically, it is strictly related to the activity of the eccrine sweat glands (located in the palms of the hands and soles of the feet) and the skin pore size. In the literature, EDR is widely used to estimate the affective state, especially when the arousal level changes. Many studies over the years have indicated that the magnitude of the electrodermal change and the intensity of emotional experience are almost linearly associated in arousal dimension [45], [70], [71].

In the literature, several approaches are used to measure this signal. In this work, a small continuous voltage is applied to the skin and the induced current is measured through two Ag/AgCl electrodes positioned at the index and middle fingertips of the nondominant hand. The ratio between voltage drop and induced current represents the skin electric impedance.

The EDR can be split into two components: tonic and phasic. The tonic component is the baseline level of skin conductance (also called skin conductance level—SCL), whose trend is different from person to person and depends on both patient physiological state and autonomic regulation. The phasic component (also called Skin Conductance Responses—SCRs), superimposed on the tonic baseline level, changes with specific external stimuli such as lights, sounds, smells, etc. The scientific community has accepted considering the EDR as an indirect indicator of the sympathetic nervous system [72].

3 Methodology

A block diagram of the proposed recognition system is illustrated in Fig. 3. After the IAPS elicitation, all signals were preprocessed, i.e., segmented and filtered. Afterward, the most significant features were extracted and then reduced using the Principal Component Analysis (PCA) method. Finally, features were classified using various machine learning methods [73]. In particular, we tested several classifiers such as Linear Discriminant Classifier (LDC), Mixture Of Gaussian (MOG), k-Nearest Neighbor (k-NN), Kohonen Self Organizing Map (KSOM), Multilayer Perceptron (MLP), and QDC. Among these, QDC showed the highest recognition accuracy and consistency in both arousal and valence multiclasses. According to that and for the sake of brevity we will report and discuss here only results from the QDC.

3.1 Preprocessing

Raw data were collected from biosensors in ASCII format and preprocessed. Each signal was segmented according to time duration of the stimulating sections (see Fig. 2).

3.1.1 Heart Rate Variability (HRV)

ECG was prefiltered through a Moving Average Filter (MAF) in order to extract and subtract the baseline. Since HRV refers to the change over time of the Heart Rate (HR), a QRS complex detection algorithm was used. Automatic QRS detection is still an open issue which can be addressed through several methods. The choice depends on the characteristics of the specific ECG signal [74], e.g., signal-to-noise-ratio (SNR), signal power, ECG leads. We adopted an automatic algorithm developed by Pan and Tompkins [75].

The interval between two successive QRS complexes is defined as the RR interval (t_{R-R}) and the heart rate (beats per minute) is given as

$$HR = \frac{60}{t_{R-R}}. \quad (1)$$

As heart rate is a time series sequence of nonuniform RR intervals, this signal was further resampled according to the algorithm of Berger et al. [76].

In addition, Independent Component Analysis (ICA) was applied to extract and remove Respiration Sinus Arrhythmias (RSA) [77].

3.1.2 Respiration

In this phase, the respiratory signal was treated in order to remove the baseline and reject the movement artifacts. Baseline removal was performed by means of MAF technique similarly to the ECG signal. Moreover, it was filtered by means of a tenth order low-pass FIR filter with a cutoff frequency of 1 Hz approximated by Butterworth polynomial.

3.1.3 Electrodermal Response

EDRs were filtered by means of a 2.5 Hz low-pass FIR filter approximated by Butterworth polynomial. As reported in the literature, we considered that the bulk of the energy of the tonic component of the signal was in the frequency band from 0 to 0.05 Hz, and the energy of the phasic component was in the band from 0.05 to 1-2 Hz [78]. Therefore, we have chosen Wavelet filtering, which is one of the best available nonstationary data analysis tools. In detail, 12 levels wavelet decomposition was applied in order to obtain tonic and phasic signals using Daubechies five function. Approximation at level 1 was the tonic component and details were the phasic component.

3.2 Feature Sets

In this work, all the features were calculated for each neutral session as well as for each A_i session. Sets of features can be extracted in different ways. In this work, we used two big categories of features: The first one consisted of most standard commonly used features, and the second category consisted of features extracted from nonlinear dynamic techniques. In this work, 89 standard features and

TABLE 4
Feature Sets

Feature set	Analysis	Signals
Standard	Time domain (MNN, SDNN, RMSSD, pNN50, TINN)	HRV
	Frequency domain (VLF, LF, HF, LF/HF)	HRV
	Frequency domain (Power in 0-0.1 Hz, 0.1-0.2 Hz, 0.2-0.3 Hz, 0.3-0.4 Hz, Central Frequency)	RSP, EDR
	Statistics (SEM, RSPR, MFD, SDFD, MSD, SDSD, SDBA, MAXRSP, MINRSP, DMMRSP, Skewness, Kurtosis)	RSP, EDR
	Statistics (Max Peak, Latency, MAD, MDNV, PNSDAS)	Phasic EDR
	High Order Spectra (MBI, VBI, MMB, PEB, NBE, NBSE)	HRV, RSP, EDR
NonLinear Methods	Deterministic Chaos (m, Δ)	HRV, RSP, EDR
	Recurrence Plot (DLE, RR, DET, LAM, TT, RATIO, ENTR, L_{max})	HRV, RSP, EDR
	Detrended Fluctuaction Analysis (α_1, α_2)	HRV, RSP, EDR

36 extracted from nonlinear dynamic methods were used (see Table 4).

3.2.1 Standard Feature Set

Standard features were derived from the time series, statistics, frequency domain, geometric analysis for the whole set of physiological signals. In the following sections these methods are described in detail.

Heart rate variability. Heart rate variability [67] is concerned with the analysis of the time intervals between heartbeats. Several features were extracted from this signal, both in the time and frequency domain. Time domain features included statistical parameters and morphological indexes. Defining, e.g., a time window (NN), several parameters were calculated, such as simple MNN and SDNN, which are the mean value and the standard deviation of the NN intervals, respectively. Moreover, we calculated the root mean square of successive differences of intervals (RMSSD) and the number of successive differences of intervals which differ by more than 50 ms (pNN50 percent expressed as a percentage of the total number of heartbeats analyzed).

Referring to morphological patterns of HRV, the triangular index was calculated. It was derived from the histogram of RR intervals into NN window (TINN) in which a triangular interpolation was performed. Triangular interpolation approximated the RR interval distribution by a linear function and the baseline width of this approximation (base of the triangle) was used as a measure of the HRV index. In the literature, TINN is known to be correlated with SDNN as well as being highly insensitive to artifacts and ectopic beats because they are left outside the triangle.

The time domain methods are simple and widely used, but are unable to discriminate between sympathetic and para-sympathetic activity, while an appreciable contribution is given by the frequency domain parameters. All features extracted in the frequency domain were based on the Power Spectral Density (PSD) of the HRV. Methods for the estimation of PSD may be generally classified as nonparametric (like Fourier Transform) and parametric (model-based) methods. In this work, we adopted the Autoregressive (AR) model to estimate the PSD of HRV in order to provide better frequency resolution than nonparametric method. Furthermore, conventional frequency transformation based on the Fourier transform technique is not very suitable for analyzing nonstationary signals. Considering HRV as an output process $z(n)$ of a causal, all-pole, discrete filter whose input is white noise, the AR method of order p is expressed as the following equation:

$$z(n) = -\sum_{k=1}^{p} a(k)z(n-k) + w(n), \tag{2}$$

where $a(k)$ are AR coefficients and $w(n)$ is white noise of variance equal to σ^2. The $\mathrm{AR}(p)$ model is characterized by AR parameters $\{a[1], a[2], \ldots, a[p], \sigma^2\}$.

In this work, we used the Burg method to get the AR model parameters, according to the results presented by Akaike [79], [80]. This method provided high resolution in frequency and yielded a stable AR model. Three main spectral components were distinguished in a spectrum calculated from short-term recordings: Very Low Frequency (VLF), Low Frequency (LF), and High Frequency (HF) components. It is well known in the literature that the distribution of the spectral power changes follows the ANS modulation. Experience with frequency domain analysis over the past two decades strongly suggests that it represents a unique, noninvasive tool for achieving a more precise assessment of autonomic function in both the experimental and clinical settings. Available studies report the importance of HF and LF components and how their analysis per se cannot afford a precise delineation of the state of sympathetic activation. Therefore, in addition to VLF, LF, and HF power, we calculated the LF/HF Ratio which should give information about the Sympatho-Vagal balance. Physiological interpretation of lower frequency components of HRV (that is of the VLF and ULF components) warrants further elucidation. These changes may indicate a shift of sympatho-vagal balance toward sympathetic predominance and reduced vagal tone. Similar conclusions were obtained by considering the changes in the LF/HF ratio [81].

Respiration. By defining a time window W, feature set was comprised of the ReSPiration Rate (RSPR), Mean and Standard Deviation of the First (MFD and SDFD, respectively) and Second Derivative (MSD and SDSD, respectively), i.e., variation of the respiration signal, Standard Deviation of the Breathing Amplitude (SDBA), and several statistical parameters. Respiration rate was calculated as the frequency corresponding to the maximum spectral magnitude. Statistical parameters were calculated in order to characterize the differences between inspiratory and expiratory phases (range or greatest breath). These parameters included the maximum (MAXRSP) and the minimum (MINRSP) value of breathing amplitude and their difference (DMMRSP). Other measures used to quantify the asymmetries between the two respiratory phases were

obtained from the High Order Statistics (HOS). In detail, we calculated the third order statistics (i.e., Skewness), which takes into account the quantification of the asymmetry of the probability distribution, and the fourth order statistics (i.e., Kurtosis), which is a measure of the "peakedness" of the probability distribution. Moreover, another parameter was the Standard Error of the Mean (SEM), which was calculated as follows:

$$SEM = \frac{\sigma}{\sqrt{n}},$$

where σ is the standard deviation and n is the number of points within the window W. Concerning features in frequency domain, spectral power in the bandwidths 0-0.1, 0.1-0.2, 0.2-0.3, and 0.3-0.4 Hz were also calculated [82].

Electrodermal Response. Standard methods for both tonic and phasic EDR features included the same statistics applied to the RSP signal above described: rate, i.e., central frequency, mean, and standard deviation of the amplitude and statistical parameters, i.e., skewness, kurtosis, SEM, and mean and standard deviation of the first and second derivative [45]. Moreover, further features were extracted only from the phasic component of EDR. More specifically, we also calculated the maximum peak and the relative latency from the beginning of the image, Mean of Absolute of Derivative (MAD), Mean of Derivative for Negative Values (MDNV) only (mean decrease rate during decay time), Proportion of Negative Samples in the Derivative versus All Samples (PNSDAS), and spectral power in the bandwidths 0-0.1, 0.1-0.2, 0.2-0.3, and 0.3-0.4 Hz) [82].

Standard Features from Higher Order Spectra. In addition to the above-mentioned standard techniques, for all the acquired signals High Order Spectra (HOS) was also examined, which is defined as Fourier transform of moments or cumulants of order grater than two. In particular, we used the two-dimensional third order cumulant Fourier Transform, called Bispectrum [83], [84]:

$$B(f_1, f_2) = \int \int_{t_1,t_2=-\infty}^{+\infty} c_3(t_1, t_2) exp^{-j(2\pi f_1 t_1 + 2\pi f_2 t_2)} dt_1 dt_2, \quad (3)$$

with the condition

$$|\omega_1|, |\omega_2| \leq \pi \quad \text{for} \quad \omega = 2\pi f.$$

The $c_3(t_1, t_2)$ variable represents the third order cumulant, which is defined as follows:

$$c_3(t_1, t_2) = E\{s(t_1)s(t_2)s(t_1 + t_2)\}, \quad (4)$$

where $s(t)$ is a square integrable stationary signal with zero mean. Thus, the bispectrum measures the correlation among three spectral peaks, ω_1, ω_2, and $(\omega_1 + \omega_2)$, and estimates the phase coupling. Sometimes the bispectrum is unable to distinguish between pairs of frequencies strongly coupled and pairs of frequency weakly coupled but at high frequencies because their bispectrum values are similar. In order to overcome this limitation, we evaluate the bicoherence function according to Brillinger et al. [85]. A previous study demonstrated that the bispectrum has several symmetry properties [84] and divides the (f_1, f_2) plane in eight symmetric zones. The bispectrum of a real signal is uniquely defined by its values in the triangular region of

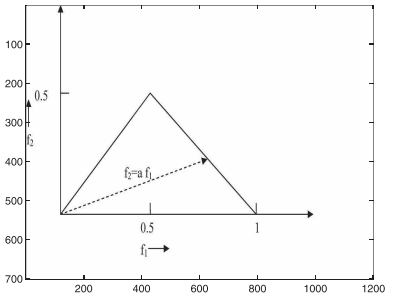

Fig. 4. Bispectrum invariants from [87].

computation, $0 \leq f_1 \leq f_2 \leq f_1 + f_2 \leq 1$, provided there is no bispectral aliasing [85]. The bispectral feature set consisted of: Mean and Variance of Bispectral Invariants (MBI and VBI), i.e., mean and variance of $P(a)$, Mean Magnitude (M_{mean}) of the Bispectrum (MMB) and the Phase Entropy P_e (PEB), Normalized Bispectral Entropy P_1 (NBE), and Normalized Bispectral Squared Entropy P_2 (NBSE). All the features were calculated within the region defined in Fig. 4, according to results presented by Chang and Sun [86] and Chua et al. [87].

3.2.2 Nonlinear Dynamic Methods for Feature Extraction

Here, we propose a new set of features extracted by nonlinear methods and applied to all the three physiological signals. A powerful technique used for analysis of complex dynamical systems is the so-called embedding procedure. Embedding of a time series $x_t = (x_1, x_2, \ldots, x_N)$ is done by creating a set of vectors X_i such that

$$X_i = [x_i, x_{i+\triangle}, x_{i+2\triangle}, \ldots, x_{i+(m-1)\triangle}], \quad (5)$$

where $\triangle$ is the delay in number of samples and m is the number of samples (dimension) of the array X_i. When embedding a time series, we must choose the dimension m of X_i and the delay Δ such that each vector X_i represents values that reveal the topological relationship between subsequent points in the time series. The number of samples in the embedded vector is usually chosen to be large enough to cover the dominant frequency in the time series, but m should not be so large that the first and last values in the epoch are practically unrelated. The evolution of the system can be represented by the projection of the vectors X_i onto a trajectory through a multidimensional space, often referred to as phase space or state space. If the trajectory is comprised within a subspace in the phase space, then this subspace is called the attractor of the system. Moreover, the Recurrence Plot (RP) [88] is a graph which shows all those times at which a state of the dynamical system recurs. In other words, the RP reveals all the times when the phase space trajectory visits roughly the same area in the phase space.

Natural processes can have a distinct recurrent behavior, e.g., periodicities (as seasonal or Milankovich cycles), but also irregular cyclicities (as El Niño Southern Oscillation). Moreover, the recurrence of states, i.e., the states are arbitrarily close after a little while, is a fundamental property of deterministic dynamical systems and is typical for nonlinear or chaotic systems. The recurrence of states in nature has been known for a long time and has also been

discussed in early publications (e.g., recurrence phenomena in cosmic-ray intensity [89]).

Eckmann et al. [90] have introduced a tool which can visualize the recurrence of states x_i in a phase space. Usually, a phase space does not have a dimension (two or three) which allows it to be pictured. Higher dimensional phase spaces can only be visualized by projection into the two or three-dimensional subspaces. However, Eckmann's tool enables us to investigate the m-dimensional phase space trajectory through a two-dimensional representation of its recurrences. When a state at time i recurs also at time j, the element (i, j) of a squared matrix NxN is set to 1, 0 otherwise. This representation is called RP. Such an RP can be mathematically expressed as

$$R_{i,j} = \Theta\big(\epsilon_i - \|x_i - x_j\|\big),$$

where $x_i \epsilon \mathbb{R}^m$, $i, j = 1, \ldots, N$; N is the number of considered states x_i, ε_i is a threshold distance, $\|.\|$ a norm, and $\Theta(.)$ the Heaviside function which is defined as

$$H(z) = \begin{cases} 1, & if \;\; z \geq 0 \\ 0, & if \;\; z < 0. \end{cases} \tag{6}$$

In this work, we chose the optimal value of ε_i [91] as follows:

$$\epsilon_i = 0.1 * A_{PD}, \tag{7}$$

where A_{PD} is averaged phase space diameter of data x_i.

Following the above description, the Recurrence Quantification Analysis (RQA) [92] is a method of nonlinear data analysis which quantifies the number and duration of recurrences of a dynamical system presented by its state space trajectory. Quantification of recurrence plots can be based either on evaluating diagonal lines to estimate chaos-order transitions or on vertical (horizontal) lines to estimate chaos-chaos transitions. In this work the following features were calculated:

Recurrence Rate (RR) is the percentage of recurrence points in an RP and it corresponds to the correlation sum

$$RR = \frac{1}{N^2} \sum_{i,j=1}^{N} R_{i,j}, \tag{8}$$

where N is the number of points on the phase space trajectory.

Determinism (DET) is the percentage of recurrence points which form diagonal lines:

$$DET = \frac{\sum_{l=lmin}^{N} lP(l)}{\sum_{i,j=1}^{N} R_{i,j}}, \tag{9}$$

where $P(l)$ is the histogram of the lengths l of the diagonal lines.

Laminarity (LAM) is the percentage of recurrence points which form vertical lines:

$$LAM = \frac{\sum_{v=vmin}^{N} vP(v)}{\sum_{v=1}^{N} vP(v)}, \tag{10}$$

where $P(v)$ is the histogram of the lengths v of the diagonal lines.

Trapping Time TT is the average length of the vertical lines:

$$TT = \frac{\sum_{v=v_{min}}^{N} vP(v)}{\sum_{v=v_{min}}^{N} P(v)}. \tag{11}$$

Ratio ($RATIO$) is the ratio between DET and RR:

$$RATIO = \frac{DET}{RR}. \tag{12}$$

Averaged diagonal line length (L) is the average length of the diagonal lines:

$$L = \frac{\sum_{l=lmin}^{N} lP(l)}{\sum_{l=lmin}^{N} P(l)}. \tag{13}$$

Entropy ($ENTR$) is the Shannon entropy of the probability distribution of the diagonal line lengths $p(l)$:

$$ENTR = -\sum_{l=lmin}^{N} p(l) \ln p(l). \tag{14}$$

Longest diagonal line (L_{max}) is the length of the longest diagonal line:

$$L_{max} = max(\{l_i; i = 1, \ldots, N_l\}), \tag{15}$$

where N_l is the number of diagonal lines in the recurrence plot.

In addition, in this work we used Detrended Fluctuation Analysis (DFA), which is a method for determining the statistical self-affinity of a signal. It is useful for analyzing time series that appear to be long-memory processes (diverging correlation time, e.g., power-law decaying autocorrelation function). It is related to measures based upon spectral techniques such as autocorrelation and Fourier transform. The DFA method has proven useful in revealing the extent of long-range correlations in time series [93]. Briefly, the time series to be analyzed (with N samples) was first integrated. Next, the integrated time series was divided into boxes of equal length, n. In each box of length n, a least squares line was fit to the data (representing the trend in that box). The y coordinate of the straight line segments is denoted by $y_n(k)$.

Next, we detrended the integrated time series, $y(k)$, by subtracting the local trend, $y_n(k)$, in each box. The root-mean-square fluctuation of this integrated and detrended time series was calculated by

$$F(n) = \sqrt{\frac{1}{N} \sum_{k=1}^{N} [y(k) - y_n(k)]^2}. \tag{16}$$

3.3 Feature Reduction Strategy

In this work, the high-dimensional feature space obtained was strictly related to the large number of features calculated by all techniques applied to the signals. Hence, a feature reduction strategy was adopted for diminishing this dimension. In the literature, two main categories of reduction methods are present, i.e., feature selection and feature projection, and these two categories comprise a large amount of algorithms. We implemented the Principal Component Analysis method, which belong to the class of

feature projection. The PCA method is able to project high-dimensional data to a lower dimensional space with a minimal loss of information. It means that new features are created by a linear transformation of original feature values, rather than by selecting a feature subset from a given feature set. A PCA description, in detail, is reported below.

3.3.1 Principal Component Analysis

PCA [94] is a useful statistical technique that projects a correlated high-dimensional space of variables to an uncorrelated low-dimensional space of variables. These variables are ordered according to decreasing variance and are called principal components. PCA uses the eigenvalues and eigenvectors generated by the correlation matrix to rotate the original data set along the direction of maximum variance. Accordingly, we have implemented the above general description by means of the Singular Value Decomposition (SVD). For the data set matrix X, of dimension $n \times p$ and rank r, it can be rewritten using SVD as

$$X = U * S * V^T, \tag{17}$$

where U is an orthogonal $n \times r$ matrix, V is an orthogonal $p \times r$ matrix with the eigenvectors $(e_1, e_2, \ldots, e_r)$, and S is the $r \times r$ diagonal matrix containing the square roots of the eigenvalues of the correlation matrix $X^T X$ and hence the variances of the Principal Components. The r eigenvectors, i.e., Principal Components of matrix V, form an orthogonal basis that spans a new vector space, called the feature space. Therefore, each vector can be projected to a single point in this r-dimensional feature space. However, according to the theory of PCA for highly correlated data, each training set vector can be approximated by taking only the first few k, where $k \leq r$, Principal Components. This mathematical method is based on the linear transformation of the different variables in principal components which could be assembled in clusters.

3.4 Classification

In this work, a Quadratic Bayes Normal Classifier (also called Quadratic Discriminant Classifier (QDC)) is used. It is parametric and based on Bayesian Decision Theory, and allowed us to minimize the overall risk, guaranteeing the lowest average error rate.

After the training process, the performance of the classification task is commonly evaluated using the confusion matrix. The generic element r_{ij} of the confusion matrix indicates how many times in percentage a pattern belonging to the class i was classified as belonging to the class j. A more diagonal confusion matrix corresponds to a higher degree of classification. The matrix has to be read by columns. The training phase is carried out on 80 percent of the feature data set (subset from 28 subjects) while the testing phase is the remaining seven subjects. We performed 40-fold cross-validation steps in order to obtain unbiased classification results, i.e., it allowed us to consider the distribution of classification results to be Gaussian, which can therefore be described as the mean and standard deviation among the 40 confusion matrix obtained. Below, the classifier is described in detail.

3.4.1 QDC

QDC [95] is a statistical-based classifier which uses a supervised learning method which determines the parameters based on available knowledge.

We assume that the input training data are a finite set $\Gamma\{(x_1, y_1), \ldots, (x_l, y_l)\}$ containing pairs of observations $x_i \in R^n$ and corresponding class labels $y_i \in Y$. Basically, statistical classifiers use *discriminant functions* $f_y(x), \forall y \in Y = \{1, 2, \ldots, c\}$ for c classes input data set and x is a *d-component* feature vector. The classifier is said to assign a feature vector x to class y_i if

$$f_i(x) > f_j(x) \qquad \forall\, j \neq i. \tag{18}$$

Thus, the classifier is viewed as a network or machine that computes c discriminant functions and selects the category corresponding to the largest discriminant. A Bayes-based classifier is easily and naturally represented in this way. For the general case with risks, we can let $f_i(x) = -R(\alpha_i|x)$ since the maximum discriminant function will then correspond to the minimum conditional risk. For the minimum-error-rate case, we can simplify things further by taking $f_i(x) = P(y_i|x)$ so that the maximum discriminant function corresponds to the maximum posterior probability.

The effect of any decision rule is to divide the feature space into c decision regions, $\Re_1, \ldots, \Re_c$. If $f_i(x) > f_j(x)\ \forall j \neq i$, then x is in region $\Re_1$ and the decision rule calls for us to assign x to f_i. The regions are separated by decision boundaries, surfaces in feature space where ties occur among the largest discriminant functions.

The structure of a Bayes classifier is determined by the conditional densities $P(x|y_i)$ as well as by the prior probabilities, according to the Bayes theorem:

$$P(y_i|x) = \frac{P(x|y_i)P(y_i)}{P(x)}, \tag{19}$$

where $P(y_i)$ and $P(x)$ are the prior probabilities.

Assuming that the minimum-error-rate classification can be achieved by using the discriminant functions [95],

$$f_i(x) = \ln P(x|y_i) + \ln P(y_i). \tag{20}$$

If the densities $P(x|y_i)$ are multivariate normal, i.e., $P(x|y_i) \sim N(\mu_i, \Sigma_i)$, where μ_i is the *d-component* mean vector and Σ_i is the *d-by-d* covariance matrix, we obtain

$$\begin{aligned} f_i(x) = &-\frac{1}{2}(x - \mu_i)^t \Sigma_i^{-1}(x - \mu_i) \\ &-\frac{d}{2}\ln 2\pi - \frac{1}{2}\ln|\Sigma_i| + \ln P(y_i), \end{aligned} \tag{21}$$

where $(x - \mu_i)^t$ is the transpose of $(x - \mu_i)$ matrix. In the general multivariate normal case, the covariance matrices are different for each category. The only term that can be dropped from the above equation is the $\frac{d}{2}\ln 2\pi$ term, and the resulting discriminant functions are inherently quadratic:

$$f_y(x) = x^t \cdot A_y x + b_y x + c_y, \qquad \forall y \in Y,$$

which are quadratic with respect to the input vector $x \in R^n$. The quadratic discriminant function f_y is determined by

TABLE 5
Confusion Matrix of QDC Classifier for Arousal Level Recognition Based on Standard Feature Set Reduced by PCA Algorithm to 12 Components

QDC	Neutral	Arousal1	Arousal2	Arousal3	Arousal4
Neutral	**98.5714±1.7795**	35.2381±16.6655	40.4762±20.2321	22.8571± 17.8350	24.2857±19.1846
Arousal1	0.3571± 1.0897	**37.1429± 17.4359**	6.6667± 8.9830	3.3333± 6.1455	6.1905± 8.9437
Arousal2	0.3571±1.0897	13.8095±13.2551	**22.3810± 18.2574**	27.6190± 20.8656	25.7143± 18.5316
Arousal3	0.1190 ±0.6521	6.6667± 8.9830	20.4762 ± 20.0924	**20.9524± 19.3974**	24.2857± 18.0507
Arousal4	0.5952±1.3537	7.1429 ± 11.0974	10.0000 ±12.5272	25.2381 ± 23.0299	**19.5238±18.1802**

TABLE 6
Confusion Matrix of QDC Classifier for Arousal Level Recognition Based on Features Extracted from Nonlinear Methods Reduced by PCA Algorithm to Seven Components

QDC	Neutral	Arousal1	Arousal2	Arousal3	Arousal4
Neutral	**100.0000±0.0000**	0.0000±0.0000	0.0000±0.0000	0.0000±0.0000	0.0000±0.0000
Arousal1	0.0000±0.0000	**100.0000±0.0000**	0.0000±0.0000	0.0000±0.0000	0.0000±0.0000
Arousal2	0.0000±0.0000	0.0000±0.0000	**92.8571±10.7295**	0.0000±0.0000	4.6429±8.7929
Arousal3	0.0000±0.0000	0.0000±0.0000	5.3571±8.3660	**82.8571±14.1754**	19.2857±16.6693
Arousal4	0.0000±0.0000	0.0000±0.0000	1.7857±4.7847	17.1429±14.1754	**76.0714±16.9302**

TABLE 7
Confusion Matrix of QDC Classifier for Valence Level Recognition Based on Standard Feature Set Reduced by PCA Algorithm to 12 Components

QDC	Neutral	Valence1	Valence2	Valence3	Valence4
Neutral	**28.5714±18.5396**	41.4286±22.6589	18.5714± 16.7755	27.8571±15.7006	22.1429±18.8128
Valence1	27.1429±14.5834	**12.8571±14.5834**	5.0000± 8.3878	16.4286±19.8138	3.5714±7.8589
Valence2	9.2857±14.1155	4.2857 ±11.4474	**22.8571± 12.6083**	14.2857±13.1095	17.1429±12.7775
Valence3	27.8571±15.7006	34.2857± 24.2614	15.0000± 12.6720	**28.5714±17.9509**	28.5714± 15.3722
Valence4	7.1429±8.6711	7.1429± 10.8698	38.5714± 16.7755	12.8571± 13.0273	**28.5714± 14.6568**

TABLE 8
Confusion Matrix of QDC Classifier for Valence Level Recognition Based on Features Extracted from Nonlinear Methods Reduced by PCA Algorithm to 13 Components

QDC	Neutral	Valence1	Valence2	Valence3	Valence4
Neutral	**96.7857±7.5783**	3.9286±6.4600	0.0000±0.0000	0.0000±0.0000	0.0000±0.0000
Valence1	3.2143±7.5783	**96.0714±6.4600**	0.0000±0.0000	0.0000±0.0000	0.0000±0.0000
Valence2	0.0000±0.0000	0.0000±0.0000	**87.1429±11.1129**	0.0000±0.0000	18.5714±11.2996
Valence3	0.0000±0.0000	0.0000±0.0000	0.0000±0.0000	**100.0000±0.0000**	0.0000±0.0000
Valence4	0.0000±0.0000	0.0000±0.0000	12.8571±11.1129	0.0000±0.0000	**81.4286±11.2996**

$$A_y = -\frac{1}{2}\Sigma_i^{-1}, \tag{22}$$

$$b_y = \Sigma_i^{-1}\mu_i, \tag{23}$$

$$c_y = -\frac{1}{2}\mu_i^t\Sigma_i^{-1}\mu_i - \frac{1}{2}\ln|\Sigma_i| + \ln P(y_i). \tag{24}$$

Of course, if the distributions are more complicated, the decision regions can be even more complex, though the same underlying theory holds there too.

4 Results

Our goal was to test the capability of the classifier to discriminate between arousal and valence along with the neutral elicitation by comparing results when only standard features and only features extracted from nonlinear dynamic methods were applied. Experimental results are shown in the form of confusion matrices and reported in Tables 5, 6, 7, and 8. The principal diagonal represents the percentage of the successful recognition of each class. More specifically, Tables 5 and 6 show the results of the four classes of different arousal (Arousal1, Arousal2, Arousal3, and Arousal4) along with the neutral one (Neutral), while Tables 7 and 8 report the results of the four classes of valence (Valence1, Valence2, Valence3, and Valence4) in addition to the neutral class (Neutral). In Tables 5 and 7, results of the QDC applied to standard features are shown, while in Tables 6 and 8, classification results are based on features extracted from nonlinear dynamic methods. These tables were obtained through the cross-validation technique, which was an average of 40 confusion matrices calculated on a randomly shuffled data set. Each element of the principal diagonal of all matrices is reported as mean value and standard deviation of the classification result. All the other elements out of the principal diagonal represent the error of classification.

Each principal component, obtained from applying the PCA algorithm to the feature sets, accounts for a given amount of the total variance. We stopped the reduction process when the cumulative variance reached 95 percent. Therefore, the number of principal components was different for standard data set and data set from nonlinear

techniques and for arousal and valence (see the table titles for further details).

5 Discussion and Conclusion

This work aimed at showing the possibility of recognizing five levels of arousal (including one neutral level) and five levels of valence (including one neutral level as well) in 35 healthy volunteers who were presented with sets of elicitation images gathered from the IAPS. The results showed that the classification through standard features were acceptable only for the neutral class, while all arousal and valence classes were misclassified. These results highlight that standard feature sets were insufficient to discriminate closed levels of arousal or valence. On the contrary, when extracted features from nonlinear dynamic methods were considered, the classification process was able to recognize each level of arousal and valence as well as the neutral class. Accordingly, good classification results are only supported by nonlinear derived features, which provide an important contribution to the state of the art, wher affective state recognition ise usually performed with much less granularity.

Results are very satisfactory, although in order to have more statistical significance the number of subjects could be increased. This problem is partially overcome by doing a cross validation in the classification process, i.e., randomizing the subjects for the training and test sets. It makes the classification independent of the sequence of the subjects involved. In addition, the 40 steps of cross validation make the distributions of the results Gaussian and explainable with only two parameters (mean and variance), as reported in all the tables. When the classifier is applied to features extracted from nonlinear dynamic methods, results are much higher than those standards and in some cases, such as Neutral and Arousal1 for arousal level recognition and Valence3 for valence level recognition we obtained full successful recognition (100 percent). A possible explanation of these results could be found in the intrinsic nonlinear behavior of the physiological responses, although the issue is inevitably open. The literature reports many attempts to find out correspondences between nonlinear dynamic systems and physiological responses, but often they are only mathematical tricks far from a clear physiological interpretation [96], [97]. Our findings only demonstrated the importance of nonlinear temporal patterns for emotion recognition [98], [99], but without claiming any specific theory. Moreover, our findings are consistent with Scherer's theory, which argues that synchronization of periodic systems is fundamental to emotion [100]. Following from this, future works could be oriented to the study of cross recurrence by means of a cross Recurrence Plot, especially between EDR and HRV.

Acknowledgments

This research is partially supported by the EU Commission under contract FP7-ICT-247777 Psyche.

References

[1] J. Russell and J.M. Carroll, "On the Bipolarity of Positive and Negative Affect," *Psychological Bull.,* vol. 125, no. 1, pp. 3-30, 1999.

[2] D. Watson, D. Wiese, J. Vaidya, and A. Tellegen, "The Two General Activation Systems of Affect: Structural Findings, Evolutionary Considerations, and Psychobiological Evidence," *J. Personality and Social Psychology,* vol. 76, no. 5, pp. 820-838, 1999.

[3] D. Watson and L. Clark, "On Traits and Temperament: General and Specific Factors of Emotional Experience and Their Relation to the Five-Factor Model," *J. Personality,* vol. 60, no. 2, pp. 441-476, 1992.

[4] C. Darwin, *The Expression of the Emotions in Man and Animals; with an Introduction, Afterword, and Commentaries by Paul Ekman.* Oxford Univ. Press, 1872.

[5] P. Ekman, "Universal Facial Expressions of Emotion," *Culture and Personality: Contemporary Readings,* p. 8, Aldine Pub. Co., 1974.

[6] P. Ekman, "Basic Emotions," *Handbook of Cognition and Emotion,* pp. 45-60, John Wiley & Sons, 1999.

[7] S. Tompkins, *Affect Imagery Consciousness: The Positive Affects,* vol. 1. Springer Publishing Company, 1962.

[8] C. Izard, *The Face of Emotion,* vol. 23. Appleton-Century-Crofts, 1971.

[9] R. Plutchik, "Emotions: A General Psychoevolutionary Theory," *Approaches to Emotion,* pp. 197-219, L. Erlbaum Assoc., 1984.

[10] P. Ekman, "Cross-Cultural Studies of Facial Expression," *Darwin and Facial Expression: A Century of Research in Review,* pp. 169-222, Academic Press, 1973.

[11] J. Watson, *Behaviorism.* Transaction Publishers, 1997.

[12] A. Ortony and T. Turner, "What Is Basic about Basic Emotions," *Psychological Rev.,* vol. 97, no. 3, pp. 315-331, 1990.

[13] W. Wundt, *Grundriss der Psychologie [Fundamentals of Psychology],* seventh rev. ed. Engelman, 1905.

[14] H. Schlosberg, "Three Dimensions of Emotion," *Psychological Rev.,* vol. 61, no. 2, pp. 81-88, 1954.

[15] C. Osgood, *The Measurement of Meaning.* Univ. of Illinois Press, 1975.

[16] J. Davitz, *The Language of Emotion.* Academic Press, 1969.

[17] P. Lang, M. Bradley, and B. Cuthbert, "Emotion, Motivation, and Anxiety: Brain Mechanisms and Psychophysiology," *Biological Psychiatry,* vol. 44, no. 12, pp. 1248-1263, 1998.

[18] J. Panskepp, *Affective Neuroscience: The Foundations of Human and Animal Emotions.* Oxford Univ. Press, 1998.

[19] C. Breazeal, "Emotion and Sociable Humanoid Robots," *Int'l J. Human-Computer Studies,* vol. 59, nos. 1/2, pp. 119-155, 2003.

[20] J. Russell, "A Circumplex Model of Affect," *J. Personality and Social Psychology,* vol. 39, no. 6, pp. 1161-1178, 1980.

[21] J. Russell and A. Mehrabian, "Evidence for a Three-Factor Theory of Emotions* 1," *J. Research in Personality,* vol. 11, no. 3, pp. 273-294, 1977.

[22] M. Arnold, *An Excitatory Theory of Emotion.* McGraw-Hill, 1950.

[23] N. Frijda, *The Emotions.* Cambridge Univ. Press, 1986.

[24] A. Ortony, G. Clore, and A. Collins, *The Cognitive Structure of Emotions,* Cambridge Univ. Press, 1990.

[25] K. Scherer and P. Ekman, *Approaches to Emotions.* Lawrence Erlbaum Assoc., Publisher, 1984.

[26] C. Lisetti and P. Gmytrasiewicz, "Can a Rational Agent Afford to Be Affectless? A Formal Approach," *Applied Artificial Intelligence,* vol. 16, pp. 1-33, 2002.

[27] K. Scherer, A. Schorr, and T. Johnstone, *Appraisal Processes in Emotion: Theory, Methods, Research,* Oxford Univ. Press, 2001.

[28] A. Egges, S. Kshirsagar, and N. Magnenat-Thalmann, "A Model for Personality and Emotion Simulation," *Proc. Knowledge-Based Intelligent Information and Eng. Systems,* pp. 453-461, 2003.

[29] J. Posner, J. Russell, and B. Peterson, "The Circumplex Model of Affect: An Integrative Approach to Affective Neuroscience, Cognitive Development, and Psychopathology," *Development and Psychopathology,* vol. 17, no. 3, pp. 715-734, 2005.

[30] L. Bialoskorski, J. Westerink, and E. Broek, "Mood Swings: An Affective Interactive Art System," *Proc. Third Int'l Conf. Intelligent Technologies for Interactive Entertainment,* pp. 181-186, 2009.

[31] C. Lisetti and F. Nasoz, "Using Noninvasive Wearable Computers to Recognize Human Emotions from Physiological Signals," *J. Applied Signal Processing,* vol. 2004, pp. 1672-1687, 2004.

[32] J. Kim and E. André, "Emotion Recognition Based on Physiological Changes in Music Listening," *IEEE Trans. Pattern Analysis and Machine Intelligence,* vol. 30, no. 12, pp. 2067-2083, Dec. 2008.

[33] J. Janssen, E. Van den Broek, and J. Westerink, "Personalized Affective Music Player," *Proc. Third Int'l Conf. Affective Computing and Intelligent Interaction and Workshops,* pp. 1-6, 2009.

[34] Y. Lin, C. Wang, T. Jung, T. Wu, S. Jeng, J. Duann, and J. Chen, "EEG-Based Emotion Recognition in Music Listening," *IEEE Trans. Biomedical Eng.,* vol. 57, no. 7, pp. 1798-1806, July 2010.

[35] E. Van den Broek, M. Schut, J. Westerink, and K. Tuinenbreijer, "Unobtrusive Sensing of Emotions (USE)," *J. Ambient Intelligence and Smart Environments,* vol. 1, no. 3, pp. 287-299, 2009.

[36] E. Van den Broek and J. Westerink, "Considerations for Emotion-Aware Consumer Products," *Applied Ergonomics,* vol. 40, no. 6, pp. 1055-1064, 2009.

[37] Z. Zeng, M. Pantic, G. Roisman, and T. Huang, "A Survey of Affect Recognition Methods: Audio, Visual, and Spontaneous Expressions," *IEEE Trans. Pattern Analysis and Machine Intelligence,* vol. 31, no. 1, pp. 39-58, Jan. 2009.

[38] K. Poels and S. Dewitte, "How to Capture the Heart? Reviewing 20 Years of Emotion Measurement in Advertising," *J. Advertising Research,* vol. 46, no. 1, p. 18, 2006.

[39] E. Leon, G. Clarke, V. Callaghan, and F. Sepulveda, "A User-Independent Real-Time Emotion Recognition System for Software Agents in Domestic Environments," *Eng. Applications of Artificial Intelligence,* vol. 20, no. 3, pp. 337-345, 2007.

[40] G. Chanel, J. Kierkels, M. Soleymani, and T. Pun, "Short-Term Emotion Assessment in a Recall Paradigm," *Int'l J. Human-Computer Studies,* vol. 67, no. 8, pp. 607-627, 2009.

[41] J. Healey, "Affect Detection in the Real World: Recording and Processing Physiological Signals," *Proc. Third Int'l Conf. Affective Computing and Intelligent Interaction and Workshops,* pp. 1-6, 2009.

[42] J. Healey and R. Picard, "Detecting Stress during Real-World Driving Tasks Using Physiological Sensors," *IEEE Trans. Intelligent Transportation Systems,* vol. 6, no. 2, pp. 156-166, June 2005.

[43] P. Lang, M. Bradley, and B. Cuthbert, "International Affective Picture System IAPS): Digitized Photographs, Instruction Manual and Affective Ratings," Technical Report A-6, Univ.of Florida, 2005.

[44] P. Lang, M. Bradley, and B. Cuthbert, "International Affective Picture System (IAPS): Technical Manual and Affective Ratings," *NIMH Center for the Study of Emotion and Attention,* 1997.

[45] P. Lang, M. Greenwald, M. Bradley, and A. Hamm, "Looking at Pictures: Affective, Facial, Visceral, and Behavioral Reactions," *Psychophysiology,* vol. 30, no. 3, pp. 261-273, 1993.

[46] P. Lang et al., "Behavioral Treatment and Bio-Behavioral Assessment: Computer Applications," *Technology in Mental Health Care Delivery Systems,* pp. 119-137, Ablex Pub. Corp., 1980.

[47] S. Grimm, C. Schmidt, F. Bermpohl, A. Heinzel, Y. Dahlem, M. Wyss, D. Hell, P. Boesiger, H. Boeker, and G. Northoff, "Segregated Neural Representation of Distinct Emotion Dimensions in the Prefrontal Cortex—An fMRI Study," *Neuroimage,* vol. 30, no. 1, pp. 325-340, 2006.

[48] A. Hariri, V. Mattay, A. Tessitore, F. Fera, and D. Weinberger, "Neocortical Modulation of the Amygdala Response to Fearful Stimuli," *Biological Psychiatry,* vol. 53, no. 6, pp. 494-501, 2003.

[49] R. Picard, E. Vyzas, and J. Healey, "Toward Machine Emotional Intelligence: Analysis of Affective Physiological State," *IEEE Trans. Pattern Analysis and Machine Intelligence,* vol. 23, no. 10, pp. 1175-1191, Oct. 2001.

[50] C. Lisetti and F. Nasoz, "Using Noninvasive Wearable Computers to Recognize Human Emotions from Physiological Signals," *EURASIP J. Applied Signal Processing,* vol. 2004, pp. 1672-1687, 2004.

[51] A. Haag, S. Goronzy, P. Schaich, and J. Williams, "Emotion Recognition Using Bio-Sensors: First Steps towards an Automatic System," *Affective Dialogue Systems,* vol. 1, pp. 36-48, 2004.

[52] K. Kim, S. Bang, and S. Kim, "Emotion Recognition System Using Short-Term Monitoring of Physiological Signals," *Medical and Biological Eng. and Computing,* vol. 42, no. 3, pp. 419-427, 2004.

[53] S. Yoo, C. Lee, Y. Park, N. Kim, B. Lee, and K. Jeong, "Neural Network Based Emotion Estimation Using Heart Rate Variability and Skin Resistance," *Proc. First Int'l Conf. Advances in Natural Computation,* pp. 818-824, 2005.

[54] A. Choi and W. Woo, "Physiological Sensing and Feature Extraction for Emotion Recognition by Exploiting Acupuncture Spots," *Proc. First Int'l Conf. Affective Computing and Intelligent Interaction,* pp. 590-597, 2005.

[55] L. Li and J. Chen, "Emotion Recognition Using Physiological Signals," *Pro. 16th Int'l Conf. Advances in Artificial Reality and Tele-Existence,* pp. 437-446, 2006.

[56] P. Rani, C. Liu, N. Sarkar, and E. Vanman, "An Empirical Study of Machine Learning Techniques for Affect Recognition in Human-Robot Interaction," *Pattern Analysis & Applications,* vol. 9, no. 1, pp. 58-69, 2006.

[57] P. Rainville, A. Bechara, N. Naqvi, and A. Damasio, "Basic Emotions Are Associated with Distinct Patterns of Cardiorespiratory Activity," *Int'l J. Psychophysiology,* vol. 61, no. 1, pp. 5-18, 2006.

[58] J. Zhai and A. Barreto, "Stress Detection in Computer Users Based on Digital Signal Processing of Noninvasive Physiological Variables," *Proc. IEEE 28th Ann. Int'l Conf. Eng. in Medicine and Biology Soc.,* pp. 1355-1358, 2006.

[59] C. Liu, K. Conn, N. Sarkar, and W. Stone, "Physiology-Based Affect Recognition for Computer-Assisted Intervention of Children with Autism Spectrum Disorder," *Int'l J. Human-Computer Studies,* vol. 66, no. 9, pp. 662-677, 2008.

[60] C. Katsis, N. Katertsidis, G. Ganiatsas, and D. Fotiadis, "Toward Emotion Recognition in Car-Racing Drivers: A Biosignal Processing Approach," *IEEE Trans. Systems, Man, and Cybernetics, Part A: Systems and Humans,* vol. 38, no. 3, pp. 502-512, May 2008.

[61] G. Yannakakis and J. Hallam, "Entertainment Modeling through Physiology in Physical Play," *Int'l J. Human-Computer Studies,* vol. 66, no. 10, pp. 741-755, 2008.

[62] C. Katsis, N. Katertsidis, and D. Fotiadis, "An Integrated System Based on Physiological Signals for the Assessment of Affective States in Patients with Anxiety Disorders," *Biomedical Signal Processing and Control,* vol. 6, pp. 261-268, 2011.

[63] R. Kohavi and F. Provost, "Glossary of Terms," *Machine Learning,* vol. 30, pp. 271-274, 1998.

[64] F. van der Heiden, R. Duin, D. de Ridder, and D. Tax, *Classification, Parameter Estimation, State Estimation: An Engineering Approach Using MatLab.* Wiley, 2004.

[65] A. Schlogl, "Time Series Analysis—A Toolbox for the Use with Matlab," 2002.

[66] K. Kroenke, R. Spitzer, and J. Williams, "The phq-9," *J. General Internal Medicine,* vol. 16, no. 9, pp. 606-613, 2001.

[67] U. Rajendra Acharya, K. Paul Joseph, N. Kannathal, C. Lim, and J. Suri, "Heart Rate Variability: A Review," *Medical and Biological Eng. and Computing,* vol. 44, no. 12, pp. 1031-1051, 2006.

[68] A. Lanata, E. Scilingo, E. Nardini, G. Loriga, R. Paradiso, and D. De-Rossi, "Comparative Evaluation of Susceptibility to Motion Artifact in Different Wearable Systems for Monitoring Respiratory Rate," *IEEE Trans. Information Technology in Biomedicine,* vol. 14, no. 2, pp. 378-386, Mar. 2010.

[69] W. Winton, L. Putnam, and R. Krauss, "Facial and Autonomic Manifestations of the Dimensional Structure of Emotion* 1," *J. Experimental Social Psychology,* vol. 20, no. 3, pp. 195-216, 1984.

[70] P. Lang, "The Emotion Probe," *Am. Psychologist,* vol. 50, no. 5, pp. 372-385, 1995.

[71] H. McCURDY, "Consciousness and the Galvanometer," *Psychological Rev.,* vol. 57, no. 6, pp. 322-327, 1950.

[72] P. Venables and M. Christie, "Electrodermal Activity," *Techniques in Psychophysiology,* pp. 3-67, Wiley, 1980.

[73] A. Jain and R. Mao, "Statistical Pattern Recognition: A Review," *IEEE Trans. Pattern Analysis and Machine Intelligence,* vol. 22, no. 1, pp. 4-37, Jan. 2000.

[74] B. Kohler, C. Hennig, and R. Orglmeister, "The Principal of Software QRS Detection," *IEEE Eng. in Medicine and Biology,* vol. 6, no. 1, pp. 42-57, Jan./Feb. 2002.

[75] J. Pan and W. Tompkins, "A Real-Time QRS Detection Algorithm," *IEEE Trans. Biomedical Eng.,* vol. 32, no. 3, pp. 230-236, Mar. 1985.

[76] R. Berger, S. Akselrod, D. Gordon, and R. Cohen, "An Efficient Algorithm for Spectral Analysis of Heart Rate Variability," *IEEE Trans. Biomedical Eng.,* vol. 33, no. 9, pp. 900-904, Sept. 1986.

[77] S. Tiinanen, M. Tulppo, and T. Seppänen, "RSA Component Extraction from Heart Rate Signal by Independent Component Analysis," *Proc. Computers in Cardiology,* pp. 161-164, 2010.

[78] A. Ishchenko and P. Shev'ev, "Automated Complex for Multiparameter Analysis of the Galvanic Skin Response Signal," *Biomedical Eng.,* vol. 23, no. 3, pp. 113-117, 1989.

[79] H. Akaike, "Fitting Autoregressive Models for Prediction," *Annals of the Inst. of Statistical Math.,* vol. 21, no. 1, pp. 243-247, 1969.

[80] A. Boardman, F. Schlindwein, A. Rocha, and A. Leite, "A Study on the Optimum Order of Autoregressive Models for Heart Rate Variability," *Physiological Measurement,* vol. 23, pp. 325-336, 2002.

[81] A. Camm et al., "Heart Rate Variability: Standards of Measurement, Physiological Interpretation, and Clinical Use," *Circulation,* vol. 93, no. 5, pp. 1043-1065, 1996.
[82] S. Koelstra, A. Yazdani, M. Soleymani, C. Mühl, J. Lee, A. Nijholt, T. Pun, T. Ebrahimi, and I. Patras, "Single Trial Classification of EEG and Peripheral Physiological Signals for Recognition of Emotions Induced by Music Videos," *Proc. Int'l Conf. Brain Informatics,* pp. 89-100, 2010.
[83] J. Mendel, "Tutorial on Higher-Order Statistics (Spectra) in Signal Processing and System Theory: Theoretical Results and Some Applications," *Proc. IEEE,* vol. 79, no. 3, pp. 278-305, Mar. 1991.
[84] C. Nikias, *Higher-Order Spectral Analysis: A Nonlinear Signal Processing Framework.* PTR Prentice-Hall, Inc., 1993.
[85] D.R. Brillinger, M. Rosenblatt, and P. Petropulu, "Computation and Interpretation of kth Order Spectra," *Spectral Analysis of Time Series,* pp. 189-232, Wiley, 1967.
[86] T.N. Chang and S. Sun, "Blind Detection of Photomontage Using Higher Order Statistics," *Proc. IEEE Int'l Symp. Circuits and Systems,* 2004.
[87] K. Chua, V. Chandran, U. Acharya, and C. Lim, "Cardiac State Diagnosis Using Higher Order Spectra of Heart Rate Variability," *J. Medical Eng. & Technology,* vol. 32, no. 2, pp. 145-155, 2008.
[88] N. Marwan, M. Carmen Romano, M. Thiel, and J. Kurths, "Recurrence Plots for the Analysis of Complex Systems," *Physics Reports,* vol. 438, nos. 5/6, pp. 237-329, 2007.
[89] A. Monk and A. Compton, "Review of Modern Physics," *The Am. Physical Soc.,* pp. 173-179, 1939.
[90] J. Eckmann, S. Kamphorst, and D. Ruelle, "Recurrence Plots of Dynamical Systems," *Europhysics Letters,* vol. 4, p. 973, 1987.
[91] S. Schinkel, O. Dimigen, and N. Marwan, "Selection of Recurrence Threshold for Signal Detection," *The European Physical J.-Special Topics,* vol. 164, no. 1, pp. 45-53, 2008.
[92] J. Zbilut and C. Webber Jr., *Recurrence Quantification Analysis.* Wiley Online Library, 2006.
[93] C. Peng, S. Havlin, H. Stanley, and A. Goldberger, "Quantification of Scaling Exponents and Crossover Phenomena in Nonstationary Heartbeat Time Series," *Chaos: An Interdisciplinary J. Nonlinear Science,* vol. 5, no. 1, p. 82, 1995.
[94] I. Jolliffe, *Principal Component Analysis.* Wiley Online Library, 2002.
[95] R. Duda, P. Hart, and D. Stork, *Pattern Classification.* Citeseer, 2001.
[96] K. Scherer, "Emotions are Emergent Processes: They Require a Dynamic Computational Architecture," *Philosophical Trans. Royal Soc. B: Biological Sciences,* vol. 364, no. 1535, pp. 3459-3474, 2009.
[97] V. Marmarelis, *Nonlinear Dynamic Modeling of Physiological Systems.* Wiley-IEEE Press, 2004.
[98] N. Fragopanagos and J. Taylor, "Emotion Recognition in Human-Computer Interaction," *Neural Networks,* vol. 18, no. 4, pp. 389-405, 2005.
[99] R. Cowie, E. Douglas-Cowie, K. Karpouzis, G. Caridakis, M. Wallace, and S. Kollias, "Recognition of Emotional States in Natural Human-Computer Interaction," *Multimodal User Interfaces,* pp. 119-153, Springer, 2008.
[100] D. Grandjean, D. Sander, and K. Scherer, "Conscious Emotional Experience Emerges as a Function of Multilevel, Appraisal-Driven Response Synchronization," *Consciousness and Cognition,* vol. 17, no. 2, pp. 484-495, 2008.

Gaetano Valenza graduated in biomedical engineering from the University of Pisa in 2009, and worked in the Interdepartmental Research Center "E. Piaggio" on the development and implementation of artificial intelligence algorithms for real-time signal processing, wireless transmission, and neuromorphic evolvable hardware. He pursued his research interest in high-level biomedical signal processing by studying nonlinear dynamics of central and peripheral neurosignals for emotion recognition (i.e., affective computing). The main topic of his fellowship is a multiparametric approach in multivariate analysis in subjects suffering from mental disorders that are monitored by wearable systems. He is a student member of the IEEE.

Antonio Lanatà graduated in electronic engineering from the University of Pisa in 2001. He worked on electro-active polymers for actuator systems. Currently, he is working toward the PhD degree at the University of Pisa, Italy, and he is pursuing his research work mainly in the Interdepartmental Research Center "E. Piaggio." His research is now focused on wearable systems and high-level signal processing for health status monitoring. In addition, he works on ultrasound technique and UltraWideBand radar technology. He is a member of the IEEE.

Enzo Pasquale Scilingo received the Laurea degree in electronic engineering from the University of Pisa, Italy, and the PhD degree in bioengineering from the University of Milan in 1995 and 1998, respectively. He is an assistant professor in electronic and information bioengineering at the University of Pisa. For two years he was a postdoctoral fellow with the Italian National Research Council and for two years a postdoctoral fellow in the Information Engineering Department of the University of Pisa. Currently, he is working on research work mainly at the Interdepartmental Research Center "E. Piaggio." Currently, he is a coordinator of the European project PSYCHE, FP7-ICT-24777. His research interests are in biomedical and biomechanical signal processing, modeling and control and instrumentation. He is the author of several papers in peer-reviewed journals, contributions to international conferences, and chapters in international books. He is a member of the IEEE.